

Fluctuations of energy injection rate in a shear flow

Jörg Schumacher and Bruno Eckhardt

Fachbereich Physik, Philipps-Universität, D-35032 Marburg, Germany

Abstract

We study the instantaneous and local energy injection in a turbulent shear flow driven by volume forces. The energy injection can be both positive and negative. Extremal events are related to coherent streaks. The probability distribution is asymmetric, deviates slightly from a Gaussian shape and depends on the position in shear direction. The probabilities for positive and negative injection are exponentially related, but the constant varies across the shear layer. These studies are a step towards an application of the microscopic chaotic fluctuation theorem to macroscopic properties.

1 Introduction

The application of ideas from dynamical systems theory to statistical mechanics far from equilibrium has led to a number of stimulating insights and developments [1,2,3,4,5,6,7,8]. Among them are a connection between the contraction of phase space volume and entropy production, e.g. for the derivation of Ohm's law in a Lorentz gas [4], and a chaotic version of the fluctuation-dissipation relation [6,9] for reversible systems. This latter relation allows for the possibility that phase space does not contract monotonically and that for short times even the inverse effect, a phase space expansion, is possible. However, the probability of expansion is exponentially suppressed compared to a contraction.

Several recent experimental efforts to study such a relation in macroscopic and mesoscopic systems have focussed on the energy input into these systems rather than the entropy production directly: Ciliberto and Laroche [10] extracted the buoyant energy input in turbulent Rayleigh-Bénard convection, Goldburg *et al.* [11] measured the power transferred to a liquid crystal in a chaotic regime above the electrohydrodynamic instability and Wang *et al.* [12] measured the energy change for a colloidal particle in an optical trap. Energy

input is not only experimentally more easily accessible, it is in these systems also the quantity that can take both positive and negative signs. The energy dissipation has a fixed sign and cannot fluctuate around zero. For macroscopic descriptions, such as the Navier-Stokes equation, the definite sign of the energy dissipation is connected with the large separation between the smallest scales of the fluid (of the order of the Kolmogorov length η_K) and the microscopic length scales (such as the mean free path λ): even in strongly turbulent flows we have $\eta_K \gg \lambda$ and thus a situation where the smallest fluid elements are large bodies with negligible deviations from the second law. It is only on smaller scales, as in the experiment [12], that the dissipation terms can change sign.

Strictly speaking, the theoretical results [6,9] therefore do not apply to the Navier-Stokes equation since it is not reversible. One way out in case of fluid dynamics is to modify the macroscopic equations, as in constrained Euler ensembles [13] or in isokinetic Navier-Stokes ensembles [14,15] so that the dynamics is once again reversible. However, even if the system is not reversible, as in the case of a Brownian particle, the fluctuations of energy injection show interesting behavior, as demonstrated by Farago [16].

In the following we therefore adopt the traditional Navier-Stokes equation as our starting point, take the energy uptake as observable, as in the experiments mentioned above, and embark on a numerical study of the statistics of local energy input in a turbulent shear flow and especially on the ratios of the probability density functions (PDF) for negative and positive energy injection. The relation between coherent structures and extremal injection rates will also be analyzed.

An empirical study of the statistics of energy input in macroscopic systems can be of value also in its own right, beyond the specific quest for a fluctuation dissipation relation. Recent experiments have indicated unexpected features in the global fluctuation statistics [17,18,19,20]. The results presented here thus connect to and complement other studies on volume averaged fluctuation statistics in hydrodynamic systems, such as experiments on thermal convection [10], the swirling flow experiments [18,20], or the studies of the GOY shell model in [21].

The specific system we study here is a hydrodynamic shear flow driven by volume forces. The system is a macroscopic version of the microscopic molecular dynamics simulations of shear flows in Evans *et al.* [6] that led to the discovery of the fluctuation theorem. The main differences between the microscopic and the macroscopic model are irreversibility and the absence of a thermostat in the latter. The flow is incompressible and a statistically stationary turbulent state is sustained by driving with a steady volume force $F_x(y)$. The Navier-Stokes equation then reads

$$\frac{\partial \mathbf{u}}{\partial t} + (\mathbf{u} \cdot \nabla) \mathbf{u} = -\nabla p + \nu \nabla^2 \mathbf{u} + \mathbf{F}, \quad (1)$$

$$\nabla \cdot \mathbf{u} = 0. \quad (2)$$

ν is the constant kinematic viscosity, $\mathbf{u}(\mathbf{x}, t)$ is the velocity field and $p(\mathbf{x}, t)$ is the kinematic pressure field. The equations of motion are solved in a volume V with periodic boundary conditions in x (streamwise) and z (spanwise) directions and with free-slip boundary conditions in shear direction y by means of a pseudospectral method (for more details see [22]). The rectangular slab has an aspect ratio of $2\pi : 1 : 2\pi$. The spectral resolution is $N_x \times N_y \times N_z = 256 \times 65 \times 256$ for all runs and the number of degrees of freedom (or independent Fourier modes) is about $2.5 \cdot 10^6$. With U_0 the amplitude of the laminar shear profile, $\mathbf{u}_0 = U_0 \cos(\pi y/L_y) \mathbf{e}_x$, and the width of the slab, L_y , we can define a Reynolds number $Re = U_0 L_y / \nu$; for our simulations it takes values between 500 and 6000.

We want to study the changes in the total kinetic energy density of the fluid, $e(\mathbf{x}, t) = \mathbf{u}(\mathbf{x}, t)^2 / 2$. Its evolution is governed by

$$\partial_t e + \partial_j (u_j e - \nu u_i \partial_j u_i + u_i p \delta_{ij}) = u_i F_i - \nu (\partial_i u_j)^2. \quad (3)$$

For the energy balance of the volume averaged kinetic energy, $E(t) = \langle \mathbf{u}^2 \rangle_V / 2$ the second term on the left hand side of (3) does not contribute as it contains a total divergence of a current whose surface integral vanishes for the given boundary conditions. The balance for the volume averaged kinetic energy thus reads

$$\frac{\partial E}{\partial t} = \frac{1}{V} \int_V u_x F_x \, dV - \frac{\nu}{V} \int_V (\nabla \mathbf{u})^2 \, dV = \epsilon_{in}(t) - \epsilon(t). \quad (4)$$

The energy dissipation rate $\epsilon(t)$, and its local version $\epsilon(\mathbf{x}, t) = (\nu/2)(\partial_i u_j + \partial_j u_i)^2$, are positive semi-definite (though zero values never occur in practice). Thus, energy is steadily taken out of the system and the corresponding entropy production rate, $\sigma(\mathbf{x}, t) \sim \epsilon(\mathbf{x}, t)$, is never negative. In contrast to thermostatted systems [6,14,15] the energy injection rate $\epsilon_{in}(t)$ is not synchronized to $\epsilon(t)$, the system is able to store energy for intermediate time intervals and the kinetic energy content, $E(t)$, fluctuates in time.

For the volume forces studied here the local energy injection rate becomes

$$\epsilon_{in}(\mathbf{x}, t) = u_x(\mathbf{x}, t) F_x(y) = \frac{\nu \pi^2 U_0}{L_y^2} \cos(\pi y/L_y) u_x(\mathbf{x}, t), \quad (5)$$

where $u_x(\mathbf{x}, t)$ is the streamwise velocity component. Energy that is given back to the source corresponds to negative values of ϵ_{in} .

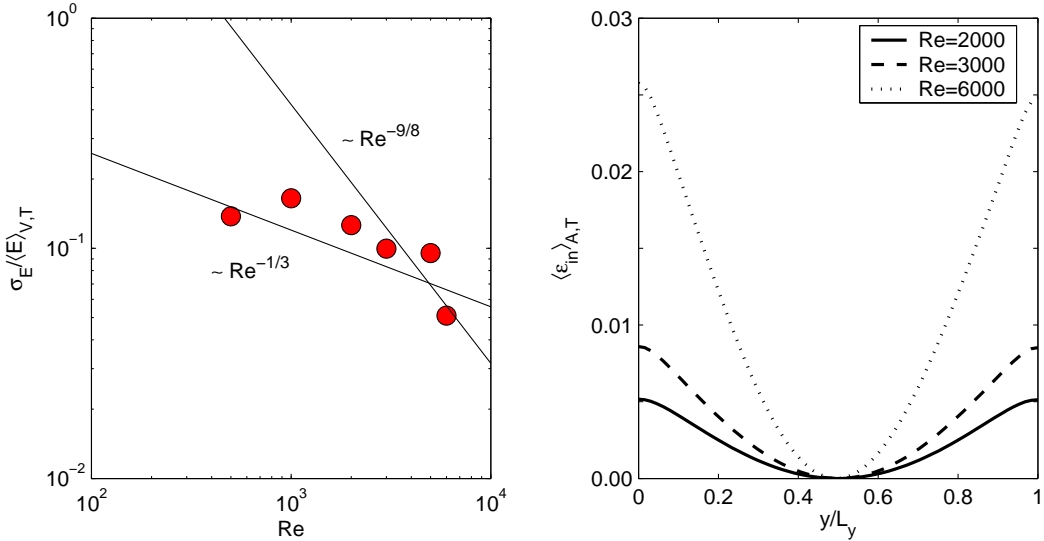


Fig. 1. Left: Ratio of standard deviation of the kinetic energy fluctuations, σ_E , and the time average, $\langle E \rangle_T = \langle \mathbf{u}^2 \rangle_{V,T}/2$ versus Reynolds number Re . Solid lines indicate the power laws with the corresponding exponents. Right: Mean energy injection rate averaged in planes $A = [0, L_x] \times [0, L_z]$ at fixed y and in time, $\langle \epsilon_{in} \rangle_{A,T}$, as a function of the shear direction y . Reynolds numbers are indicated in the legend. The particular kind of steady forcing gives rise to a y -dependent profile for the mean energy injection rate.

The variances of the fluctuations in the kinetic energy are shown for different values of the Reynolds number in Fig. 1. In addition to the volume average $\langle \cdot \rangle_V$ we will also use averages over planes at fixed y and over time. Those averages will be indicated by indices A and T , respectively. The fluctuations of volume averaged kinetic energy (left panel of Fig. 1) decrease with increasing Reynolds number. This is an indication that the increasing number of degrees of freedom that become dynamically active with increasing Reynolds number tend to average out. In quantitative terms the number of active Fourier modes outside the viscous subrange (i.e. with wave lengths exceeding the Kolmogorov scale $\eta_K = (\nu^3/\epsilon)^{1/4}$) is roughly $N \sim (L/\eta_K)^3 \sim Re^{9/4}$ [23], so that, assuming a law of large numbers, we might expect $\sigma_E \sim N^{-1/2} \sim Re^{-9/8}$. Experiments in a closed swirling turbulent flow indicated a slope $\sim Re^{-1/3}$ [18]. For the Reynolds number range accessible in our simulations no definite conclusion on either scaling can be drawn.

For the applied volume forcing the flow is not homogeneous in the shear direction, as indicated by the variations of average energy uptake with position in shear direction (right panel of Fig. 1). It is homogeneous in the downstream and the spanwise direction, so that for all statistical measures we can collect in one ensemble all points in the x - z -planes for fixed shear coordinate y .

The higher energy content of the largest scales and the prevalence of large coherent structures in shear flows [24] suggest that the energy uptake is dom-

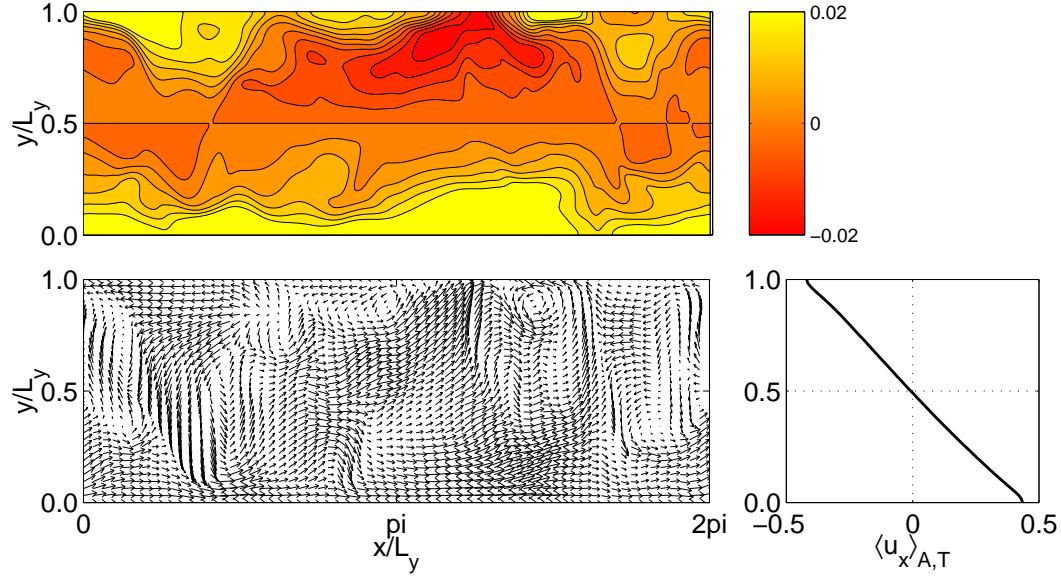


Fig. 2. Snapshot of the velocity field and the corresponding energy injection rate field at fixed position $z_0/L_y = \pi$ for the run with $Re = 6000$. The upper panel shows ϵ_{in} and the lower left panel shows u_x and u_y in a vector plot. The mean flow profile $\langle u_x \rangle_{A,T}(y)$ is indicated in the lower right. Clearly, the dark regions with negative ϵ_{in} coincide with regions where the fluid moves coherently opposite to the mean flow.

inated by large scale flows. In shear flows, the predominant structures are downstream vortices and streamwise streaks. One such event that is connected with a negative energy injection rate is shown in Fig. 2. We do observe fluid moving coherently into the opposite direction to the mean flow $\langle u_x \rangle_{A,T}(y)$ which is plotted in the lower right panel of Fig. 2.

2 Statistical analysis of the energy injection rate

The energy input can be large, both positive and negative, but it cannot be arbitrarily large. Its volume average $\epsilon_{in}(t)$ can be related to the rms velocity fluctuations by a Cauchy-Schwartz inequality

$$|\langle \epsilon_{in}(t) \rangle_T| \leq \left\langle \langle u_x^2 \rangle_V^{1/2} \langle F_x^2 \rangle_V^{1/2} \right\rangle_T = \frac{\nu \pi^2 U_0}{\sqrt{2} L_y^2} \langle u_{x,rms} \rangle. \quad (6)$$

Fluctuations exceeding the external velocity scale U_0 are extremely unlikely, so that ϵ_{in} is bounded by $\sim U_0^2$. The local energy injection rate can be estimated using the maximum norm, with a similar bound $\sim U_0^2$, but a different prefactor. For the numerical simulations both bounds turned out to be much too crude and much larger than both the maximal and the rms fluctuations

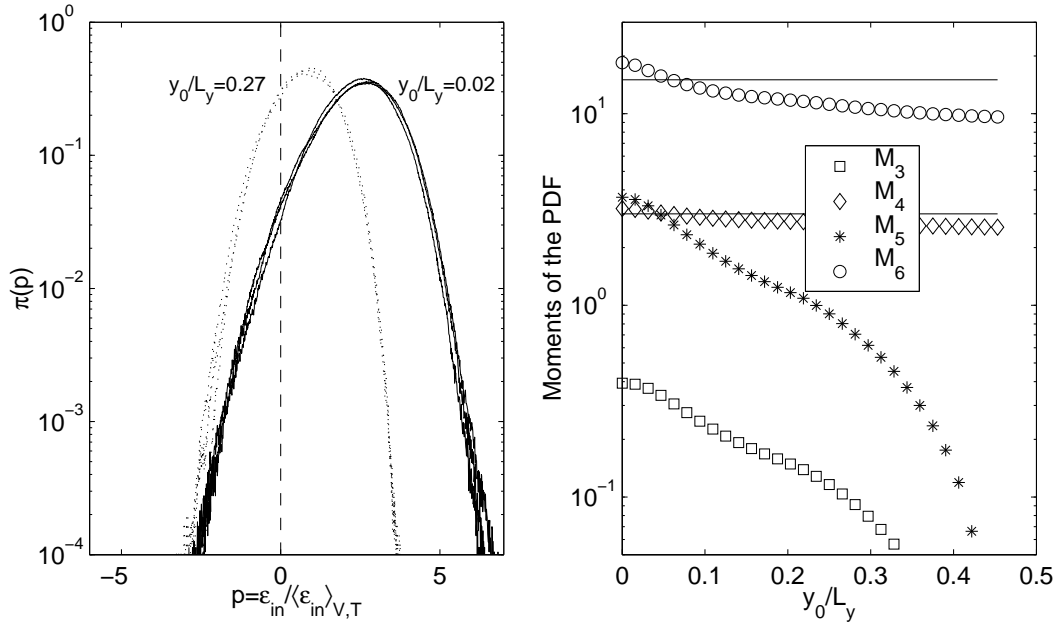


Fig. 3. Statistics of energy uptake for different vertical positions in the shear layer. Left: Probability density function (PDF) of the energy input rate. The statistics is based on about 100 turbulent snapshots separated in time by 1.5 large eddy turnover times; it contains about 6×10^8 data points. The PDF's are shown for three different Reynolds numbers, $Re = 3000, 5000$ and 6000 and the y_0 values of the fixed planes are indicated in the figure. Right: Normalized moments of ϵ_{in} versus position y_0/L_y of fixed plane. Values for a Gaussian distribution, $M_4 = 3$ and $M_6 = 15$, are indicated by solid lines. Reynolds number was 6000 .

of the downstream velocity. These bounds would thus become effective in the far tails of the probability distribution only.

We focus on the fluctuations of the instantaneous, pointwise energy injection $\epsilon_{in}(\mathbf{x}, t)$. We expect that any kind of spatial or temporal average over regions and times longer than the corresponding correlation lengths and times could push the distributions closer to Gaussian shape. It is interesting to note that this does not seem to be the case in [17,18]. But even in that case a instantaneous and local distribution should provide a more sensitive measure of possible deviations from a Gaussian shape. Since our system is invariant under translation in downstream and spanwise direction, but not in the normal direction, we study the distributions for planes parallel to the bounding surfaces separately. The probability density functions of the energy input rate in units of its ensemble average $\langle\epsilon_{in}\rangle_{V,T}$ and for different positions between the plates are shown in Fig. 3.

The collapse of the PDF's for different Reynolds numbers, rescaled by the volume averages, indicates a universality of the fluctuations of large scale injection (left panel of Fig. 3), as also observed in experiment [18,20]. The PDF we find is similar to the one measured in [20] and much closer to Gaussian

shape than the one in [18]. As a measure of deviations we determine the normalized and centered moments $M_n = \langle (p - \langle p \rangle_{A,T})^n \rangle / \langle (p - \langle p \rangle_{A,T})^2 \rangle^{n/2}$ where $\langle (p - \langle p \rangle_{A,T})^n \rangle = \int (p - \langle p \rangle_{A,T})^n \pi(p) dp$ and $p = \epsilon_{in} / \langle \epsilon_{in} \rangle_{V,T}$. In particular the ones for $n = 4$ and $n = 6$ differ from the Gaussian values of 3 and 15 which are indicated by solid lines in the right panel of Fig. 3. However, the PDF also changes when going from the free-slip side planes at $y_0/L_y = 0$ towards the center at $y_0/L_y = 1/2$: the odd moments are smaller near the center, indicating a more symmetric PDF (see right panel of Fig. 3). The PDF is closest to Gaussian here.

We next turn to the logarithm of the ratio of the probabilities for positive and negative injection rates, $\log[\pi(p)/\pi(-p)]$ where p is again a particular value of the dimensionless $\epsilon_{in}(\mathbf{x}, t) / \langle \epsilon_{in} \rangle_{V,T}$. In Fig. 4 we show

$$C_0(p) = \frac{1}{p} \log \left[\frac{\pi(p)}{\pi(-p)} \right]. \quad (7)$$

A constant C_0 indicates a linear exponential relation between the probabilities of positive and negative energy injection. As is well known the slope C_0 can be related to the mean and the variance in a Gaussian model for the fluctuations. Clearly the logarithmic ratio of the probability density functions is then automatically linear, but the value of C_0 was found to be unity in simpler systems that satisfy all the assumptions for the fluctuation theorem [8]. If the distribution has the form

$$\pi(p) = N \exp(-(p - \bar{p})^2 / 2\sigma^2), \quad (8)$$

with normalization factor N , then

$$C_0 = 2 \frac{\bar{p}}{\sigma^2} = 2 \frac{\langle \epsilon_{in} \rangle_{A,T} \langle \epsilon_{in} \rangle_{V,T}}{\langle \epsilon_{in}^2 \rangle_{A,T} - \langle \epsilon_{in} \rangle_{A,T}^2}. \quad (9)$$

In Fig. 4, we have also indicated the C_0 value as given by (9) by dashed lines. For the PDF close to the center of the flow this estimate agrees with the value from the PDF of the data, but near the side planes deviations become visible. Here the strength of energy input is largest on average and coherent flow structures are most prominent. In all cases and in agreement with Farago's investigation [16] our C_0 is larger than unity.

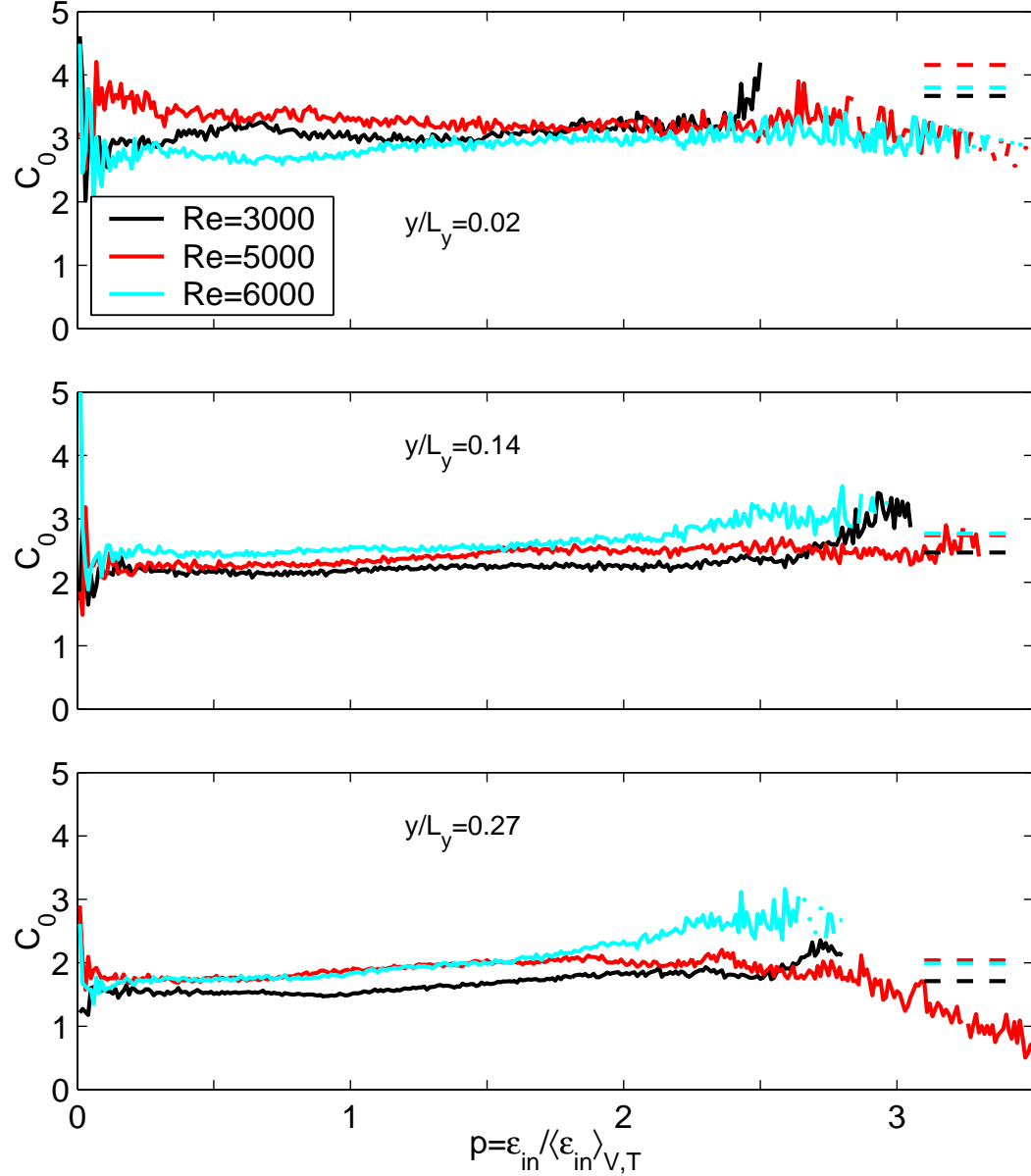


Fig. 4. Test of the linearity of the logarithmic ratio as suggested by Eq. (7). The stronger oscillations for very small p arise due to the amplification of small wiggles on the PDF $\pi(p)$ there. The linear slope is fairly independent of Re . Data are as in Fig. 3. The dashed lines on the far right indicate the values of C_0 obtained from Eq. (9).

3 Concluding remarks

We have studied the fluctuations of the energy injection rate in a turbulent shear flow for various Reynolds numbers. We considered the injection rate as a macroscopic substitute for the entropy production rate (or phase space contraction rate) that enters the fluctuation relation for microscopic

non-equilibrium systems. The mean value of the energy input rate and the shape of its probability distribution varied across the shear flow. The results did not depend much on the Reynolds number and the probability density functions collapsed when rescaled by the mean value of ϵ_{in} . The probabilities for positive and negative energy injection were found to be exponentially related over a range of more than twice the mean values. However, the constant in the exponent varies across the layer, in contrast to what would be expected from the fluctuation theorem. Thus, while there are some indications for an exponential relation between positive and negative energy uptake, the quantitative behaviour depends on the position across the layer and is not as universal as in the fluctuation relation.

As mentioned in the introduction, the Navier-Stokes equation is perhaps closest in its global features to the Brownian particle studied by Farago [16]. That model predicts a crossover to another slope for large energy uptake, but the statistical uncertainties in our numerical data are too large to study this. Other systems that might provide guidance for what to expect in the fluctuation statistics are thermostatted Lorentz gases where time reversibility is broken by a magnetic field [25].

Further avenues worth exploring include the relation between coherent structures and energy uptake or energy blocking (as in Fig. 2), and the implications for backscatter effects in turbulent flows, i.e., the phenomenon that locally energy does not cascade down to smaller but up to larger scales. This might be important for subgrid-scale modelling within large-eddy simulations [26].

Acknowledgements

We thank J. Davoudi, J. R. Dorfman, G. Gallavotti, W. I. Goldburg, W. Losert, T. Tel and J. Vollmer for useful discussions. The computations were done on a Cray SV1ex at the John von Neumann-Institut für Computing at the Forschungszentrum Jülich and we are grateful for their support. This work was also supported by the Deutsche Forschungsgemeinschaft.

References

- [1] P. Gaspard and G. Nicolis, *Phys. Rev. Lett.* 65 (1990) 1693.
- [2] D. J. Evans and G. P. Morris, *Statistical Mechanics of Non-equilibrium Liquids*, Academic Press, London 1990.
- [3] W. G. Hoover, *Computational Statistical Mechanics*, Elsevier, Amsterdam 1991.

- [4] N. I. Chernov, G. L. Eyink, J. L. Lebowitz and Ya. G. Sinai, Phys. Rev. Lett. 70, (1993) 2209.
- [5] N. I. Chernov, G. L. Eyink, J. L. Lebowitz and Ya. G. Sinai, Commun. Math. Phys. 154, (1993) 569.
- [6] D. J. Evans, E. G. D. Cohen and G. P. Moriss, Phys. Rev. Lett. 71, (1993) 2401.
- [7] J. R. Dorfman, An introduction to chaos in non-equilibrium statistical mechanics, Cambridge University Press, Cambridge 1999.
- [8] J. Vollmer, Phys. Rep. 372, (2002) 131.
- [9] G. Gallavotti and E. G. D. Cohen, Phys. Rev. Lett. 74, (1995) 2694; J. Stat. Phys. 80, (1995) 931.
- [10] S. Ciliberto and C. Laroche, J. Phys. IV France 8, (1998) 215.
- [11] W. I. Goldburg, Y. Y. Goldschmidt, and H. Kellay, Phys. Rev. Lett. 87, (2001) 245502.
- [12] G. M. Wang, E. M. Sevick, E. Mittag, D. J. Searles, and D. J. Evans, Phys. Rev. Lett. 89, (2002) 050601.
- [13] Z.-S. She and E. Jackson, Phys. Rev. Lett. 70, (1993) 1255.
- [14] L. Rondoni and E. Segre, Nonlinearity 12, (1999) 1471.
- [15] G. Gallavotti, L. Rondoni and E. Segre, *Lyapunov spectra and nonequilibrium ensembles equivalence in 2D fluid mechanics*, preprint (2002).
- [16] J. Farago, J. Stat. Phys. 107, (2002) 781.
- [17] S. T. Bramwell, P. C. W. Holdsworth and J.-F. Pinton, Nature 396, (1998) 552.
- [18] J.-F. Pinton, P. C. W. Holdsworth and R. Labb  , Phys. Rev. E 60, (1999) R2452.
- [19] A. Noullez and J.-F. Pinton, Eur. Phys. J. B 28, (2002) 231.
- [20] J. H. Titon and O. Cadot, Phys. Fluids 15, (2003) 625.
- [21] S. Aum  tre, S. Fauve, S. McNamara and P. Poggi, Eur. Phys. J. B 19, (2001) 449.
- [22] J. Schumacher and B. Eckhardt, Phys. Rev. E 63, (2001) 046307.
- [23] L. D. Landau and E. M. Lifschitz, *Course in Theoretical Physics: Fluid Mechanics*, Pergamon Press, Oxford, 1987.
- [24] J. Schumacher and B. Eckhardt, Europhys. Lett. 52, (2000) 627.
- [25] M. Dolowschi  k and Z. Kov  cs, Phys. Rev. E 66, (2002) 066217.
- [26] M. Lesieur and O. Metais, Annu. Rev. Fluid Mech. 28, (1996) 45.